IET Electric Power Applications

*Research Article*

IET Journals
The Institution of Engineering and Technology

# Space vector pulse width modulation control techniques for a five-phase quasi-impedance source inverter

ISSN 1751-8660
Received on 13th June 2017
Revised 10th October 2017
Accepted on 7th November 2017
E-First on 18th December 2017
doi: 10.1049/iet-epa.2017.0340
www.ietdl.org

*Ahmad Anad Abduallah[1], Mohammed Meraj[2], Mohammed Al-Hitmi[2], Atif Iqbal[2]* ✉

[1]*Department of Electronics and Electrical Engineering, Liverpool John Moores University, Liverpool, UK*
[2]*Department of Electrical Engineering, Qatar University, Doha, Qatar*
✉ *E-mail: atif.iqbal@qu.edu.qa*

**Abstract:** This study proposes space vector modulation (SVM) techniques for a five-phase quasi-impedance source inverter. Five different SVM methods are elaborated utilising four active neighbouring (from two different lengths group) and a zero space vector to synthesise the reference voltage with the aim of obtaining sinusoidal output voltage waveforms. The main objective of the developed SVM methods is to reduce total harmonic distortion (THD) in the output voltage waveform while simultaneously boosting the DC link voltage. Shoot-though period is computed according to the required boost in the DC voltage and spread in a switching cycle. Five different schemes are developed based on the shoot-through application in a number of inverter legs. A comprehensive comparative study of the proposed SVM techniques is carried out based on various obtained characteristics such as the shoot-through duty ratio, boost factor, voltage gain, THD and efficiency. Theoretical analysis and simulation results are validated using experimental approach.

## 1 Introduction

Multiphase adjustable speed drives are currently considered for various applications due to the inherent benefits that they offer when compared to three-phase counterpart. Some of the advantages are: reduced torque pulsation at higher frequency, reduced size and higher efficiency, lower DC link current harmonics, higher torque density, greater fault tolerance and additional degree of freedom for enhanced control performance and reduced per-leg power converter ratings [1, 2]. The multiphase machines are mainly considered for use in applications such as electric ship propulsion, more electric aircrafts, hybrid and electric vehicle, on-board charging system and traction [1, 2]. Electric machine always requires two current components (namely $d$ and $q$) to produce torque irrespective of the number of phases. Multiphase machines have additional current components that can be utilised for other purposes such as control of series [3] or parallel connected multiphase machines [4], control of DC link capacitor voltages in machines with multiple three-phase windings and multiple three-phase series-connected converters [5], and for on-battery charging for electric vehicle [6].

Multiphase drives are traditionally fed from standard two-level multiphase voltage source inverters (VSIs) [7], multiphase multilevel inverter [8] and direct AC–AC converters [9]. This paper proposes multiphase quasi-impedance source inverter (qZSI) as an option for multiphase motor drive.

The traditional two-level multiphase inverter is by nature a buck converter that outputs much lower voltage than the input. The maximum achievable value of output voltage in a $n$-phase inverter is $(0.5V_{dc}/\cos(\pi/2n))$ [10], where $V_{dc}$ is the DC link voltage and $n$ is the number of phases of inverter. It is seen that the output from inverter gets lower as the number of phases increases. Lower voltage affects the torque of the machine (torque is proportional to the square of voltage) and hence the drive is overrated for the required torque. Other problem arises due to voltage sag, which may lead to complete shutdown since the ride-through capability of the drive is poor. Ride-through can be improved by integrating additional storage devices and over rating of the drive. These solutions lead to higher cost, size/volume and complexity of the overall system. When a standard multiphase inverter is used in conjunction with the diode rectifier, it pollutes the line with distorted currents. Usually, the dead time is used to avoid shoot-through (shorting of the inverter leg) in traditional inverter control. This causes unstable operation of the drive at low speed and introduced distortion in the output voltage waveform. Shoot-through is not allowed in conventional inverters and the same is employed for the useful purpose of boosting the source voltage in qZSI. The proposed inverter topology bears the advantage of a single-stage inverter used for boosting and inverting the DC source voltage. The ride-through capability of the drive can be improved without additional hardware and improve the power quality by reducing the harmonic current [11, 12].

The ZSI and qZSI are attractive for use in solar photovoltaic applications due to boosting feature in a single-stage conversion [13–15]. Nevertheless, they are also considered for variable speed induction motor (IM) and synchronous motor drives applications [16–19] and electric/hybrid electric vehicle applications [20, 21] exploiting the boosting characteristics and offering the aforementioned advantages. Most of the literature available on qZSI-based motor drives is limited to three-phase systems. There are only a few publications related to multiphase qZSI [22–24]. Carrier-based pulse-width modulation (PWM) scheme is developed for five-phase qZSI with switched inductor in [22]. Continuous space vector PWM technique is developed in [23], however, the reported space vector PWM is carried out using only two large lengths vectors and hence the output voltages contain low-order harmonics. Space vector PWM with four adjacent vectors were introduced in [23], illustrating only one scheme. Discontinuous space vector PWM method is elaborated in [24] aimed at reduced switching losses and two different schemes were reported.

This paper proposes five-phase qZSI for motor drives application with the aim of obtaining a solution that encompasses the advantages of qZSI and multiphase systems. Space vector PWM techniques are developed for a five-phase qZSI by using four adjacent vectors in each sector and switching between these four vectors for specific times. Shoot-through period is applied in either one, two, three, four or all five legs and accordingly five different space vector modulation (SVM) schemes are designed and reported.

Five-phase qZSI supplying five-phase motor drive system is shown in Fig. 1 and different symbols used are as follows: $V_{in}$ is the DC source voltage, $v_{dc}$ is the DC link peak voltage, $I_{dc}$ is the DC side current, $P_{out}$ is the AC output power, $V_{ac}$ is the AC phase-

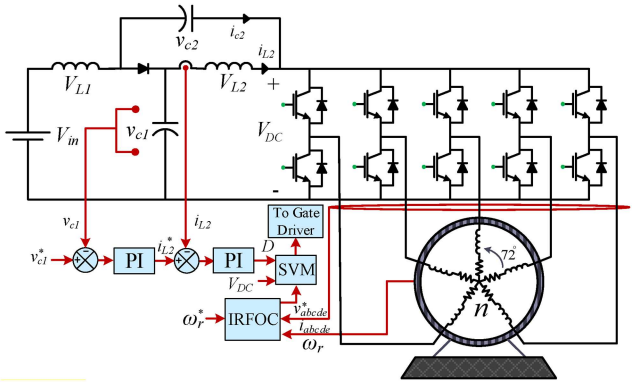


**Fig. 1** *Five-phase qZSI fed five-phase IM*

to-neutral root-mean-square (RMS), $v_{ac}$ is the AC phase-to-neutral peak voltage, $I_{ac}$ is the AC RMS current, $i_{ac}$ is the AC peak current, $D$ is the shoot-through duty ratio, $m$ is the modulation index, $B$ is the boost factor, $G$ is the voltage gain.

## 2 Quasi-Z-source inverter operation

The operation of a qZSI can be elaborated from two switching states called, the shoot-through state (one or more legs are shorted, i.e. both upper and lower switches are on simultaneously) and the non-shoot-through state (normal switching). During the non-shoot-through state, the inverter works as a current source while it becomes a voltage source during shoot-through state [13]. The shoot-through state interchanges with the non-shoot-through state; the shoot-through state is accomplished by utilising part of the zero state or the whole zero state to boost the input of the DC voltage source. The capacitor $C_1$ is selected equal to the capacitor $C_2$ and inductor $L_1$ is selected equal to inductor $L_2$ in the qZS network. The voltage across capacitors $C_1$ and $C_2$ and current through inductors ($L_1$ and $L_2$) are functions of shoot-through duty ratio $D$ and are given as follows [14, 15]:

$$V_{C1} = \frac{1-D}{1-2D}V_{in} \tag{1}$$

$$V_{C2} = \frac{D}{1-2D}V_{in} \tag{2}$$

$$I_{L1} = \frac{1-D}{1-2D}I_{dc} = I_{L2} \tag{3}$$

The DC link peak voltage is given in (4) and the AC peak voltage is presented in (5)

$$v_{dc} = \frac{1}{1-2D}V_{in} = BV_{in} \tag{4}$$

$$V_{AC} = m \cdot B\frac{V_{in}}{2} \tag{5}$$

The boosting factor is obtained as

$$B = \frac{1}{1-2D} \tag{6}$$

$$D = \frac{B-1}{2B} \tag{7}$$

$$D = \frac{T_{sh}}{T_s}, \quad T_{sh} = D \cdot T_s \tag{8}$$

$$G = m \cdot B \tag{9}$$

The voltages in (1) and (2) are the average voltages. Also, the current in (3) is the average current passing through the qZS inductor [13]. The shoot-through duty ratio is the shoot-through period over the switching period, where $T_s$ is the switching period and $T_{sh}$ is the shoot-through period.

## 3 SVM of a five-phase qZSI

The switching operation of a five-phase VSI yield 32 voltage space vectors (30 are active and 2 are zero), spans in ten sectors with sector span of $\pi/5$. The obtained voltage vectors can be grouped into three sets depending on their length, namely 'large' ($(2/5)2\cos(\pi/5)V_{dc}$), 'medium' ($(2/5)V_{dc}$) and 'small' ($(2/5)2\cos(2\pi/5)V_{dc}$), forming three concentric decagons [25]. These vectors are decomposed into two planes namely $\alpha$–$\beta$ and $x$–$y$. The outer decagon space vectors of the $\alpha$–$\beta$ plane map into the inner decagon of the $x$–$y$ plane, the innermost decagon of $\alpha$–$\beta$ plane forms the outer decagon of the $x$–$y$ plane, while the middle decagon space vectors map into the same region. Furthermore, the above mapping shows that the phase sequence $a$, $b$, $c$, $d$, $e$ of the $\alpha$–$\beta$ plane corresponds to $a$, $c$, $e$, $b$, $d$ sequence of the $x$–$y$ plane [25].

While implementing space vector PWM, four adjacent vectors (two large and two medium) and one zero vector are used respecting the volt-second principle [25] with the aim of producing sinusoidal output voltages. The space vector PWM for a five-phase two-level inverter is well established [2]. The dwell time expressions used in standard two-level five-phase VSI are reproduced here to keep consistency [25]

$$T_{al} = T_s \cdot \sigma \cdot k \cdot \sin\left(\frac{\pi}{5}j - \theta\right) \tag{10}$$

$$T_{am} = T_s \cdot \sigma \cdot \sin\left(\frac{\pi}{5}j - \theta\right) \tag{11}$$

$$T_{bl} = T_s \cdot \sigma \cdot k \cdot \sin\left(\theta - (j-1)\frac{\pi}{5}\right) \tag{12}$$

$$T_{bm} = T_s \cdot \sigma \cdot \sin\left(\theta - (j-1)\frac{\pi}{5}\right) \tag{13}$$

$$\sigma = \frac{5|V_s^*|}{2V_{dc} \cdot \sin(\pi/5)} \tag{14}$$

$$k = |v_l|/|v_m| = 1.618 \tag{15}$$

$$T_0 = T_s - T_{al} - T_{bl} - T_{am} - T_{bm} \tag{16}$$

where $j$ is the sector number ($j = 1 \ldots 10$) and $V^*_s$ is the reference voltage, $k$ is the ratio of the large and medium space vectors lengths and $\theta$ is the position of the reference voltage vector. The dwell times $T_{al}$, $T_{bl}$, $T_{am}$, $T_{bm}$ and $T_0$ have their usual meanings [25].

In a quasi-$Z$-source inverter, there exists an additional switching state, called shoot-through state. During shoot-through the two switches of the same leg are turned on simultaneously. This causes boosting of the DC source voltage that appears at the input of the inverter and subsequently converted as AC output.

In the proposed space vector PWM of five-phase qZSI, the number and location of shoot-through periods are varied in a switching period in order to obtain different schemes. Five different space vector PWM schemes are possible by introducing either 1, 2,3, 4 or 5 shoot-through periods within a switching period, accordingly named as SVQ$i$($i \in 1, 2, 3, 4, 5$) as shown in Fig. 2. Alternatively, the number in suffix is same as the number of inverter legs in which shoot-through is applied. Here it is important to highlight the difference between five-phase and standard three-phase qZSI. Five-phase qZSI offers a higher flexibility of control compared to three-phase counterpart because of a large number of legs.

It is important to note that the shoot-through dwell time depends on the number of legs where shoot-through is introduced, e.g. in SVQ5 the total shoot-through dwell time is divided equally into ten equal periods per switching cycle. Furthermore, each

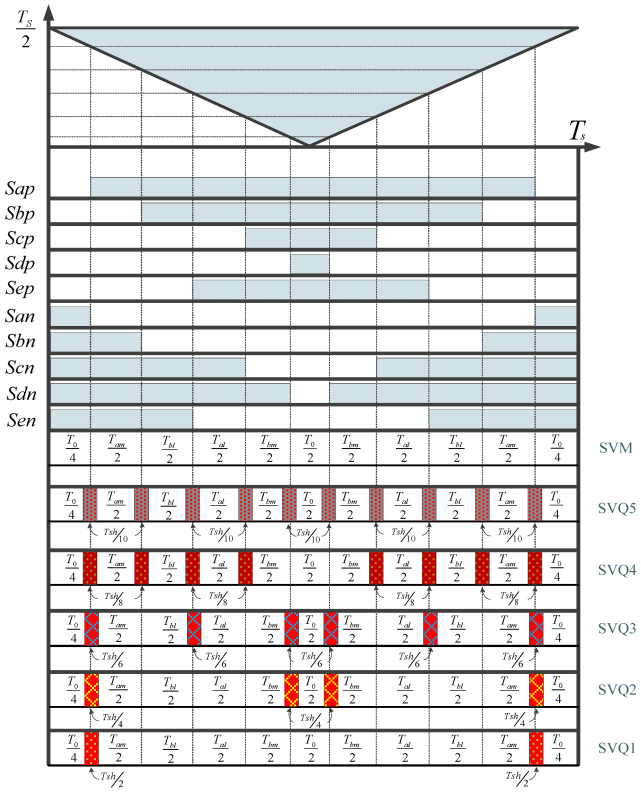


**Fig. 2** *Switching pattern for five-phase VSI and qZSI for different modulation schemes (SVM, SVQ5, SVQ4, SVQ3, SVQ2 and SVQ1)*

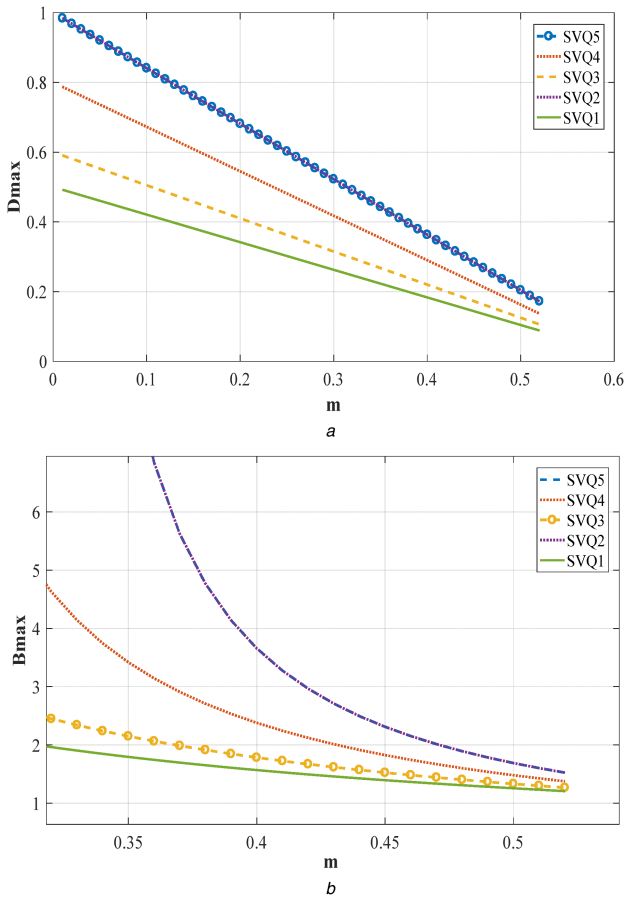


**Fig. 3** *Maximum shoot-through duty ratio and the maximum boost factor*
***(a)*** Maximum shoot-through duty ratio versus the modulation index ($m <= 0.5257$), ***(b)*** Maximum boost factor versus the modulation index

**Table 1** Maximum shoot-through duty ratio, maximum boost factor and maximum gain for SVQ*i* schemes with large and medium space vectors

| | $D_{max}$ | $B_{max}$ | $G_{max}$ |
|---|---|---|---|
| SVQ5 | $1-\frac{1.91}{\pi}\sigma\cdot(1+k)$ | $\frac{\pi}{3.82\sigma\cdot(1+k)-\pi}$ | $\frac{\pi\cdot\sigma}{3.82\sigma\cdot(1+k)-\pi}$ |
| SVQ4 | $\frac{4}{5}-\frac{1.53}{\pi}\sigma\cdot(1+k)$ | $\frac{\pi}{3.06\sigma\cdot(1+k)-0.6\pi}$ | $\frac{\pi\cdot\sigma}{3.06\sigma\cdot(1+k)-0.6\pi}$ |
| SVQ3 | $\frac{3}{5}-\frac{1.14}{\pi}\sigma\cdot(1+k)$ | $\frac{\pi}{2.28\sigma\cdot(1+k)-0.2\pi}$ | $\frac{\pi\cdot\sigma}{2.28\sigma\cdot(1+k)-0.2\pi}$ |
| SVQ2 | $1-\frac{1.91}{\pi}\sigma\cdot(1+k)$ | $\frac{\pi}{3.82\sigma\cdot(1+k)-\pi}$ | $\frac{\pi\cdot\sigma}{3.82\sigma\cdot(1+k)-\pi}$ |
| SVQ1 | $\frac{1}{2}-\frac{0.95}{\pi}\sigma\cdot(1+k)$ | $\frac{\pi}{1.91\sigma\cdot(1+k)}$ | $\frac{\pi}{1.91(1+k)}$ |

shoot-through period is divided equally between the upper and lower switches. In the other schemes, the shoot-through dwell time is divided into 8, 6, 4 and 2 equal periods, as shown in Fig. 2.

Switching pattern for sector I is presented in Fig. 2, where $S_{ap}$, … $S_{ep}$ and $S_{an}$, … $S_{en}$ represent switching signals for upper switches and lower switches of five-phase qZSI, respectively. The dwell time of shoot-through state is applied at the transition of switching states of each leg of the first half cycle and symmetrically repeated in the second half cycle as seen in Fig. 2. In order to minimise the effect of the shoot-through state on the control of the inverter, the maximum shoot-through period is defined equal to the average dwell time of zero vector period $\bar{T}_0$. The shoot-through period is limited to the average zero sequence period if the high-performance control is required, because having higher shoot-through period than the zero-vector period, this will affect the control of the drive. However, the affect will be smaller since the average zero state period is considered. Nevertheless, if the shoot-through period is much larger than the average zero state period, then the symmetry of the voltage and current waveforms is affected. The maximum shoot-through duty ratio is expressed in (17) and (18). The average zero state over one switching cycle for sector I is described in (18).

$$\frac{T_0}{T_s}=1-\left(\frac{T_{am}}{T_s}+\frac{T_{al}}{T_s}+\frac{T_{bm}}{T_s}+\frac{T_{bl}}{T_s}\right) \tag{17}$$

$$\begin{aligned}\frac{\bar{T}_0}{T_s}&=\frac{5}{\pi}\int_0^{\pi/5}1-\left(\frac{T_{am}}{T_s}+\frac{T_{al}}{T_s}+\frac{T_{bm}}{T_s}+\frac{T_{bl}}{T_s}\right)\mathrm{d}\theta\\&=\frac{5}{\pi}\int_0^{\pi/5}(1-\sigma(1+k)\cdot\sin\left(\frac{\pi}{5}-\theta\right)-\sigma(1+k)\cdot\sin\theta)\,\mathrm{d}\theta\\&=1-\frac{1.91}{\pi}\sigma(1+k)\end{aligned} \tag{18}$$

Using (6)–(9) and (17), (18), Table 1 describes the maximum possible shoot-through ratio ($D_{max}$), maximum boost factor ($B_{max}$) and the maximum voltage gain ($G_{max}$) for all five SVQ*i* schemes developed in this paper. By defining the limits of the maximum gain can be obtained by each scheme, the system control will not be affected by the high gains. It can be noticed from Table 1 that the maximum shoot-through duty ratio and the maximum boost factor can be obtained from SVQ5 and SVQ2 as illustrated in Fig. 3, while the least $D$ and $B$ are obtained by the SVQ1 scheme. Fig. 3 is obtained mathematically to show the relation. These are general observations and mathematical formulations to define the relation between the modulation, boost factor and shoot-through duty ratio. However, the inverter is designed to achieve a boost factor of DC link voltage of around 3.

## 4 Switching device power for SVQ$_i$ modulation methods

In order to calculate the total average power for the switches of the five-phase qZSI, a summation of the average switch power is performed as

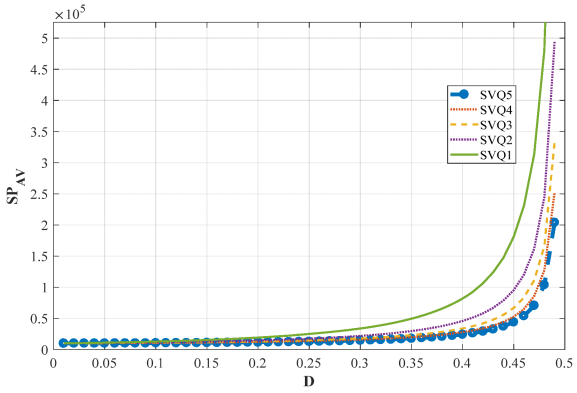


**Fig. 4** *Average switch power ($SP_{AV}$) versus shoot-through duty cycle (D) for different modulation schemes*

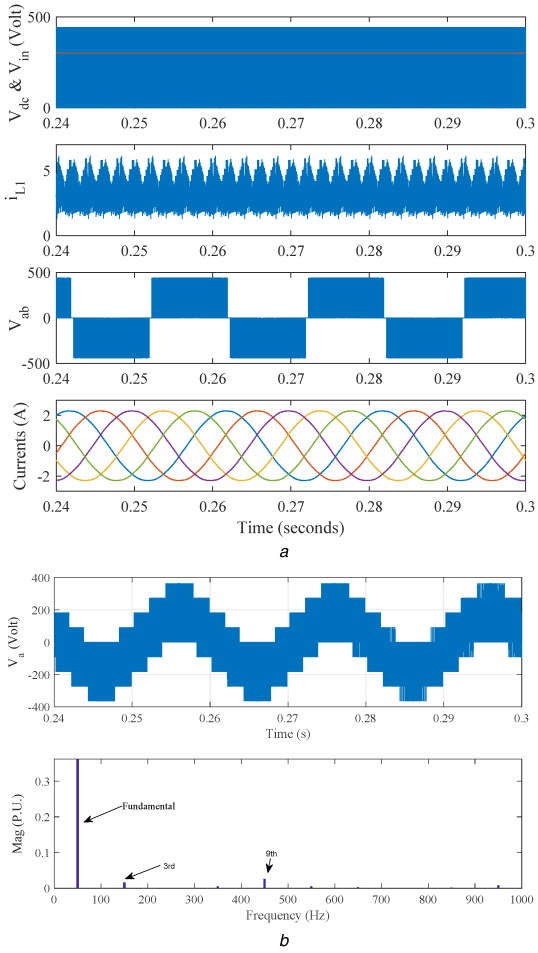


**Fig. 5** *Simulation results of SVQ5*

***(a)*** *$V_{dc}$ and $V_{in}$*, inductor current $i_{L1}$, line voltage, ***(b)*** Phase voltage ($V_a$) and its fast Fourier transform

$$SP_{AV} = \sum_{n=1}^{N} V_n I_n \tag{19}$$

where $N$ is total number of switches which is 10 in case of a five-phase qZSI while $n = 1, 2, \ldots, 10$ and $V_n$ and $I_n$ are the peak voltage and the average current through the $n$th switch [14]. $I_n$ current is a summation result of two currents, the first current is the load current $i_{ac}$ in the non-shoot-through state and the other one is current in the shoot-through state [14]. The shoot-through current consists of $2i_L$ in the positive half cycle and $(2i_L + i_{ac})$ in the negative half cycle of $i_{ac}$ [14]. The average current in the non-shoot-through state is described as

$$I_{nonAV} = \frac{1}{2\pi}\int_0^{\pi} (\sqrt{2}I_{ac}\sin\theta)\mathrm{d}\theta = \frac{\sqrt{2}I_{ac}}{\pi} \tag{20}$$

where the output power of the inverter is

$$P_{out} = 5V_{ac}I_{ac}\cos(\phi) \tag{21}$$

where

$$V_{ac} = \frac{v_{ac}}{\sqrt{2}} = \frac{mB}{2\sqrt{2}}V_{in} \tag{22}$$

The average current during the shoot-through state is represented as

$$\begin{aligned} I_{shAV} &= \frac{1}{2\pi}\int_0^{\pi} 2i_L\mathrm{d}\theta + \int_{\pi}^{2\pi}(2i_L + \sqrt{2}I_{ac}\sin\theta)\mathrm{d}\theta \\ &= 2I_L - \frac{\sqrt{2}I_{ac}}{\pi} \end{aligned} \tag{23}$$

$$I_L = P_{out}/V_{in} \tag{24}$$

The total average current flowing through the $n$th switch is as follows [14]:

$$I_n = \frac{2D}{K_{sh}}I_{shAV} + \left(1 - \frac{2D}{K_{sh}}\right)I_{nonAV} \tag{25}$$

where $K_{sh}$ is the number of switches in which shoot-through is occurring in each scheme. Substituting (19)–(24) in (25)

$$I_n = \frac{4P_{out}}{V_{in}}\left(\frac{D}{K_{sh}} + \left(1 - \frac{4D}{K_{sh}}\right)\frac{1}{5\pi mB\cos\phi}\right) \tag{26}$$

Then the switches power can be calculated as

$$\begin{aligned} SP_{AV} &= \sum_{n=1}^{N} V_n I_n \\ &= NBV_{in}I_n \\ &= 4NP_{out}\left(\frac{D}{(1-2D)K_{sh}} + \left(1 - \frac{4D}{K_{sh}}\right)\frac{1}{5\pi m\cos(\phi)}\right) \end{aligned} \tag{27}$$

Fig. 4 illustrates the $SP_{AV}$ against the shoot-through duty ratio $D$. The results show that the power stress on SVQ1 is the highest while the lowest power stress is obtained in SVQ5 for the same $D$.

## 5 Simulation results

The proposed methods are validated using Matlab/Simulink. To prove the viability of the proposed control schemes, the input DC voltage is kept at 300 V, boosting factor is chosen as 1.5 and the switching frequency is 10 kHz. Fig. 5 shows the voltage at the DC link ($V_{dc}$), the input voltage ($V_{in}$), input inductor current ($i_{L1}$), adjacent line-to-line voltage ($V_{ab}$) and the five-phase load currents. The frequency spectrum for the line-to-neutral voltage ($V_a$) is shown for SVQ5 since for this scheme the resultant voltage is almost sinusoidal and the total harmonic distortion (THD) is very small (considering up to 20th lower order harmonics). The highest harmonic is the ninth and the third, respectively, and the THD% = 1.64%. The simulation results of the SVQ4 show that the THD in $V_a$ is more than SVQ5. The second and the ninth harmonics are the highest low-order harmonics introduced in SVQ4 while the ninth harmonic is highest in SVQ5. SVQ3 has the second, third and ninth as the highest low-order harmonics and the SVQ2 has higher second harmonic than the SVQ3. The highest THD is in SVQ1 scheme, where the second, third, fourth and the sixth are the highest low-order harmonics.

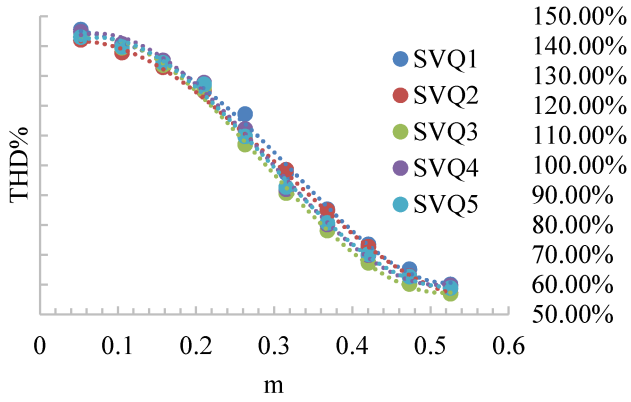


**Fig. 6** *THD% versus modulation index for different modulation schemes (SVQ5, SVQ4, SVQ3, SVQ2 and SVQ1)*

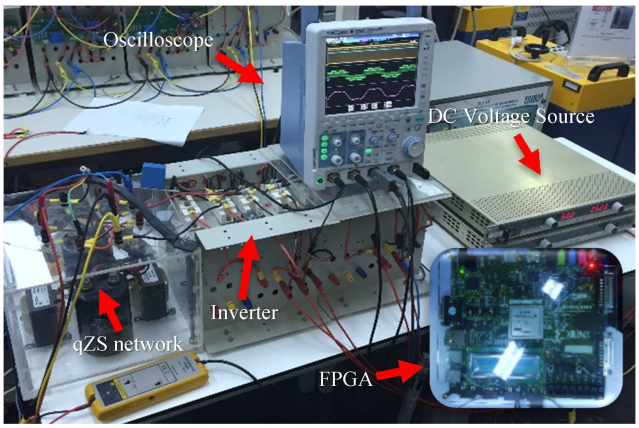


**Fig. 7** *Experimental setup*

THD is computed by considering the switching harmonics up to 25 kHz and the resulting waveform is given in Fig. 6 for different modulation indices. It is seen that the THDs are more or less the same for all the methods, with slightly better values for SVQ5. At high modulation index SVQ3 is better compared to other schemes, because of the symmetrical shoot-through switching frequency.

A further comparison is performed for the proposed SVQ schemes, based on the gain in the DC link voltage, the ripple in DC link and the low-order harmonic performance and the results are tabulated in Table 2. The highest DC link voltage gain is achieved in SVQ2 method and lowest ripple is attained in SVQ5.

## 6 Experimental results

The proposed SVQ*i* schemes are implemented and verified using experimental approach. The experimental setup is illustrated in Fig. 7 for the five-phase qZSI. The experimental setup consists of qZS network, a five-phase inverter, DC voltage source and Xilinx FPGA board (Genesys™ Virtex-5 FPGA Development Board) to control the setup. The FPGA board control code has been developed using system generator. All experiments have been tested with RL load. The qZS network is formed by two equal capacitors (2000 µF) and two equal inductors of (2.6 mH). THD analysis is performed using FLUKE power analyser. The experimental setup parameters are in Table 3.

The experiments of the SVQi schemes were performed with RL load and a switching frequency of 10 kHz. The resistor value of the RL load is 95 Ω while the inductance value is 135 mH. The test is conducted for all five-space vector PWM methods; however, the results are illustrated for two methods only, i.e. for SVQ1 and SVQ5. Fig. 8 illustrates the results of implementing the SVQ5 and SVQ1 methods. The results show the DC voltage after boosting, the input inductor current, phase output voltage, phase current and the THD% in the output voltage and current. The results indicate the boosting of the DC source voltage to 150%. The voltage and current depict acceptable THD limit. The source DC voltage, boosted DC voltage and qZ-source inductor current are shown in Fig. 9 for about three switching cycles. The non-shoot-through and shoot-through states are clearly marked. It is seen that the inductor current increases during the shoot-through state while it decreases in the non-shoot-through state. This is because of the fact that the energy is being stored in the inductor during shoot-through state while it releases during the non-shoot-through state. All the five-phase output currents for five-phase star-connected RL load are shown in Fig. 10 for SVQ5 method.

As expected from the simulation results, SVQ1 is the method with the highest harmonic distortion (THD*i* = 3.0%) and the highest DC voltage deviation. SVQ5 scheme results illustrated in Fig. 8*a* indicate that the output current is closer to sinusoidal than the other schemes and the boosting is achieved as anticipated and with a THD*i* is equal to 1.8%. The SVQ5 scheme is the best method in terms of low THD and achieving the desired DC voltage gain. The observation made by implementing the five schemes is that the harmonic distortion increases as the shoot-through state period increases or increases as the number of phases the shoot-through state implemented decreases. The reason behind this is, two of the space vectors will carry all the burden of the shoot-through state, unlike the SVQ5 where all the vectors share the burden equally. In order to achieve higher DC link voltage utilisation, less harmonic distortion, less switch voltage stress and a sinusoidal current, the best method to utilise for a five-phase qZSI is SVQ5 (Table 4).

In order to measure the power losses of the qZS network, the efficiency of the qZS network is computed experimentally. Fig. 11 illustrates the qZS network efficiency for different SVQ schemes. The results show that efficiency decreases as the shoot-through number decreases. The efficiency of qZS network increases as the number of shoot-through periods is increasing as in SVQ5, nevertheless, SVQ1 has higher efficiency in the medium power range, however, at higher power the efficiency decreases. The overall efficiency of the five-phase qZSI for different SVQ schemes is illustrated in Fig. 12. The overall efficiency of the qZSI is increasing as the shoot-through period and the input power increases, and the efficiency decreases as the number of the shoot-

**Table 2** Comparison of different SVQ*i*

| Method name | SVQ5 | SVQ4 | SVQ3 | SVQ2 | SVQ1 |
|---|---|---|---|---|---|
| gain, % | 98 | 95 | 91 | 112 | 108 |
| DC ripples range, % | 0.33 | 0.68 | 0.68 | 2.3 | 3.17 |
| highest low harmonics | ninth | secondninth | thirdninth | secondseventhninth | second, thirdfourth, sixthseventh, ninth |

**Table 3** Experimental setup parameters

| | |
|---|---|
| switching frequency | 10 kHz |
| boost factor | 1.5 |
| C1, C2 | 2000 µF |
| L1, L2 | 2.6 mH |
| R load | 95 Ω |
| L load | 135 mH |

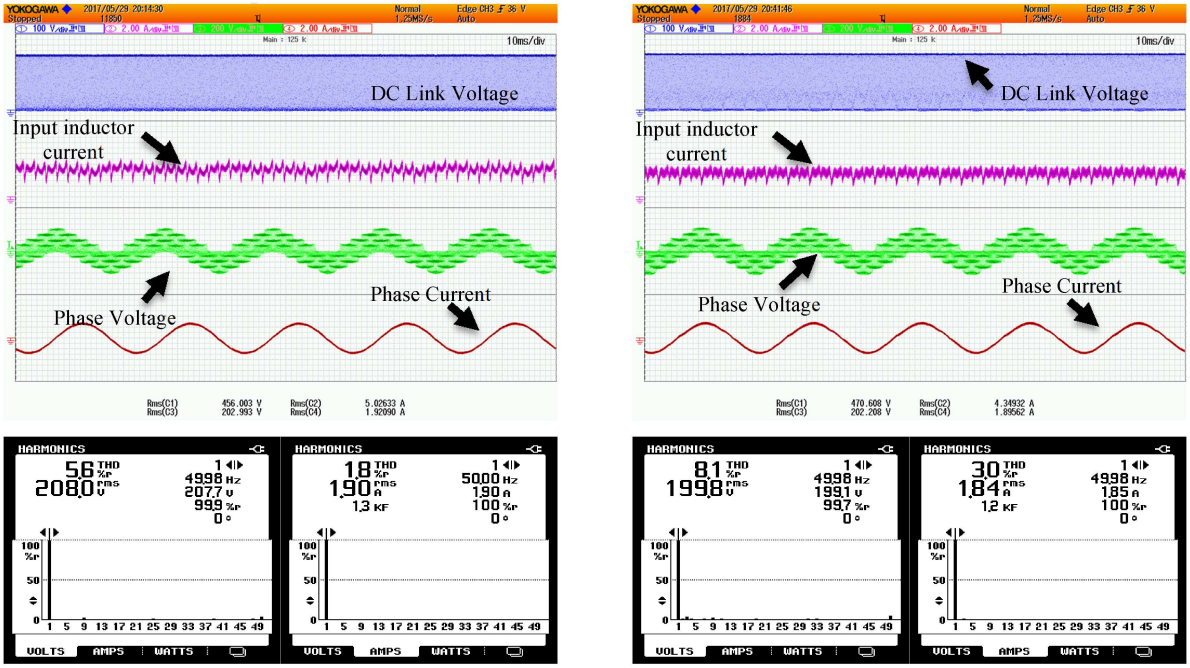


a b

**Fig. 8** *Experimental results*
**(*a*)** SVQ scheme, **(*b*)** SVQ1 scheme

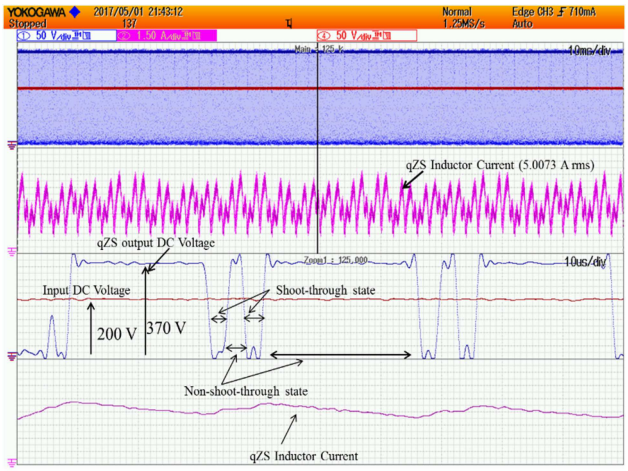


**Fig. 9** *Experimental results of SVQ5 method showing shoot-through and non-shoot-through states*

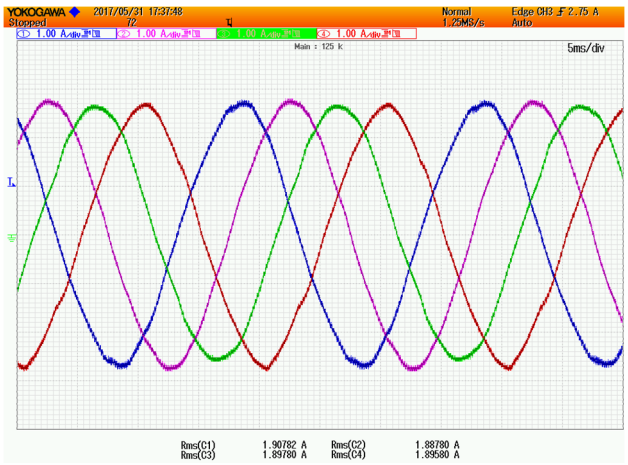

**Fig. 10** *Five-phase qZSI currents for SVQ5 method*

through period are decreasing. The efficiency of the SVQ*i* methods is subjected to a ±2% error due to the error of the current and voltage probes. The efficiency results illustrate that the SVQ5 method has the best efficiency among the five methods due to its symmetrical shoot-through period distribution.

Experimental results show the operation of a five-phase IM fed by a five-phase qZSI with space vector PWM under $v/f$ = constant

**Table 4** Low-order harmonics of different SVQ*i* obtained by experimental results

| Method name | SVQ5 | SVQ4 | SVQ3 | SVQ2 | SVQ1 |
|---|---|---|---|---|---|
| highest low-order harmonics | ninth | ninth | second, ninth | third, ninth | second, third, fourth, seventh, ninth |

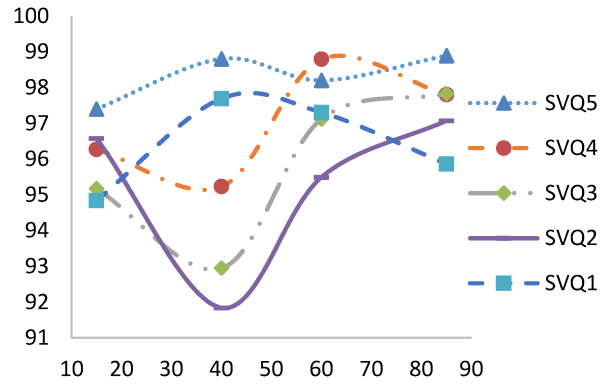


**Fig. 11** *Efficiency of the qZS network for different modulation schemes versus percentage of rated load*

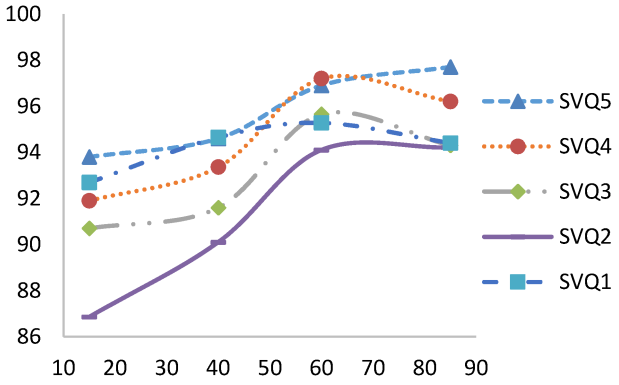


**Fig. 12** *Efficiency of the five-phase qZSI for different modulation schemes versus percentage of rated load*

**Table 5** Parameters of the five-phase IM

| Parameter | Value | Parameter | Value |
|---|---|---|---|
| $P$, kW | 2.2 | $R_r$, Ω | 15.5 |
| $V_s$, V | 230 | $L_s$, mH | 103.1 |
| $i_s$, A | 4.8 | $L_r$, mH | 92.2 |
| pole pairs | 3 | $L_m$, mH | 1356.0 |
| $N_n$, rpm | 960 | $J_m$, kg.m$^2$ | 0.007 |
| $R_s$, Ω | 25.3 | $B_m$, N m s | 0.0018 |

control scheme. The parameters of the tested five-phase IM are given in Table 5.

Experimental results of the five-phase IM drive system are shown in Fig. 13. A linear increase in the voltage and frequency is seen in Fig. 13*a* and the time of acceleration up to the rated speed is 10 s. Figs. 13*b–d* illustrate the operation at the different frequencies such as 25, 37 and 50 Hz. To clearly show the transients some sections are zoomed and presented in Figs. 13*b–d*. The drive system shows a typical $v/f$ = constant response.

## 7 Conclusion

The paper proposes different SVM schemes for a five-phase qZSI. The proposed five-phase qZSI configuration is highly beneficial for medium-voltage high-power drives applications due to boosting capability of the DC input and subsequently inverting to AC output.

A comparison is done for the THD considering both low- and high-order harmonics, gain in the DC link and the ripple in the DC link voltage. It is found that the SVM with shoot-through in all the five legs offers better THD, achieves the desired gain and introduces lower DC link ripple. Even harmonics are generated in the output voltage waveform if shoot-through is done only in one leg. The worst method in terms of THD, as anticipated from the simulation results, is the SVQ1. The proposed (SVQ*i*) schemes for the five-phase qZSI are different from the SVM methods proposed in the literature for the three-phase ZSI since four space vectors are utilised. The time of application of the zero space vectors utilised to implement the zero-state or the shoot-through time interval, while in SVQ*i* schemes the time of application of the shoot-through is divided equally through all space vectors time intervals. The SVQ*i* shows less harmonic distortion than the other schemes. The experimental results show quite the same results as in the simulation. The observation made by implementing the five schemes using large and medium vectors is that the harmonic distortion increases as the shoot-through state period increases. The reason behind this is that two of the space vectors will carry all the burden of the shoot-through state in SVQ1, while in SVQ5 all the vectors share this burden. In order to achieve higher DC link voltage utilisation, less harmonic distortion, less switch voltage stress and a sinusoidal current, the best method to utilise for five-phase qZSI is SVQ5.

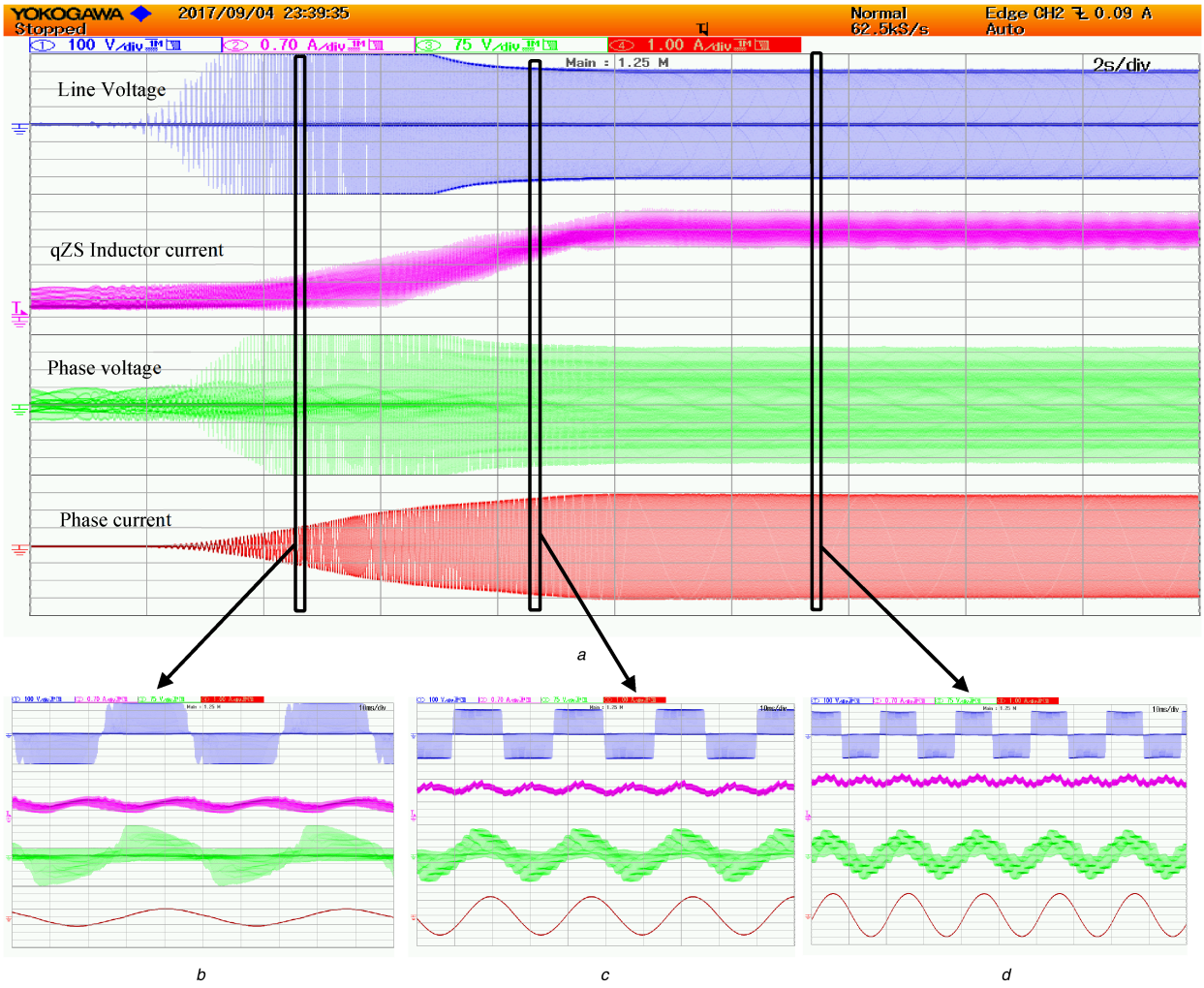


**Fig. 13** *V/f operation of the five-phase IM*

***(a)*** During start-up of IM, ***(b)*** Zoomed at frequency 20 Hz, ***(c)*** Zoomed at frequency 37 Hz, ***(d)*** Zoomed at frequency 50 Hz

## 8 References


[1] Levi, E.: 'Advances in converter control and innovative exploitation of additional degrees of freedom for multiphase machines', *IEEE Trans. Ind. Electron.*, 2016, **63**, (1), pp. 433–448

[2] Levi, E., Bodo, N., Dordevic, O., *et al.*: 'Recent advances in power electronic converter control for multiphase drive systems'. 2013 IEEE Workshop on Electrical Machines Design, Control and Diagnosis (WEMDCD), Paris, 2013, pp. 158–167

[3] Levi, E., Jones, M., Iqbal, A., *et al.*: 'Induction machine/Syn-Rel two-motor five-phase series-connected drive', *IEEE Trans. Energy Convers.*, 2007, **22**, (2), pp. 281–289

[4] Jones, M., Vukosavic, S.N., Levi, E.: 'Parallel-connected multiphase multidrive systems with single inverter supply', *IEEE Trans. Ind. Electron.*, 2009, **56**, (6), pp. 2047–2057

[5] Che, H.S., Levi, E., Jones, M., *et al.*: 'Operation of a six-phase induction machine using series-connected machine-side converters', *IEEE Trans. Ind. Electron.*, 2014, **61**, (1), pp. 164–176

[6] Subotic, I., Bodo, N., Levi, E., *et al.*: 'On-board integrated battery charger for EVs using an asymmetrical nine-phase machine', *IEEE Trans. Ind. Electron.*, 2015, **62**, (5), pp. 3285–3295

[7] Chen, K.Y., Hu, J.S.: 'A filtered SVPWM for multiphase voltage source inverters considering finite pulse-width resolution', *IEEE Trans. Power Electron.*, 2012, **27**, (7), pp. 3107–3118

[8] Govindaraju, C.: 'Efficient sequential switching hybrid modulation techniques for multiphase multilevel inverters', *IET Power Electron.*, 2011, **4**, (5), pp. 557–569

[9] Iqbal, A., Ahmed, S.K.M., Abu-Rub, H.: 'Space vector PWM technique for a three-to-five phase matrix converter', *IEEE Trans. Ind. Appl.*, 2012, **48**, (2), pp. 697–707

[10] Iqbal, A., Levi, E., Vukosavic, S.N.: 'Generalised sinusoidal PWM with harmonic injection for multi-phase VSIs', 2006 37th IEEE Power Electronics Specialists Conf., Jeju, 2006, pp. 1–7

[11] Peng, F.Z., Joseph, A., Wang, J., *et al.*: 'Z-source inverter for motor drives', *IEEE Trans. Power Electron.*, 2005, **20**, (4), pp. 857–863

[12] Liu, Y., Abu-Rub, H., Ge, B., *et al.*: 'Z-Source inverter for motor drives Application' in '*Impedance source power electronic converters*' (John Wiley & Sons, Ltd, Chichester, UK, 2016), vol. 1

[13] Peng, F.Z.: 'Z-source inverter', *IEEE Trans. Ind. Appl.*, 2003, **39**, (2), pp. 504–510

[14] Liu, Y., Boming, Ge., Abu-Rub, H., *et al.*: 'Overview of space vector modulations for three-phase Z-source/quasi-Z-source inverters', *IEEE Trans. Power Electron.*, 2014, **29**, (4), pp. 2098–2108

[15] Liu, Y., Baoming, Ge., Abu-Rub, H., *et al.*: 'A modular multilevel space vector modulation for photovoltaic quasi-Z-source cascade multilevel inverter'. IEEE Twenty-Eighth Annual Applied Power Electronics Conf. and Exposition (APEC), 2013, 17–21 March 2013, pp. 714–718

[16] Ellabban, O., Abu-Rub, H.: 'Field oriented control of a five phase induction motor fey by a Z-source inverter'. IEEE Int. Conf. on Industrial Technology (ICIT), Cape Town, 2013, pp. 1624–1629

[17] Nisha, K.C.R., Jain, S.: 'PV powered performance enhanced three-stage cascaded quasi Z-source inverter fed induction motor drive'. 2015 Int. Conf. on Circuits, Power and Computing Technologies [ICCPCT-2015], Nagercoil, 2015, pp. 1–7

[18] Dongsen, S., Baoming, G., Weiliang, W., *et al.*: 'Quasi-Z source inverter based pole-phase modulation machine drive system'. 2011 Int. Conf. on Electrical Machines and Systems, Beijing, 2011, pp. 1–6

[19] Tajima, G., Kosaka, T., Matsui, N.: 'Experimental studies on drive performances of wound field synchronous motor drive integrated with ZSI'. 2015 IEEE Applied Power Electronics Conf. and Exposition (APEC), Charlotte, NC, 2015, pp. 262–269

[20] Liu, P., Liu, H.P.: 'Permanent-magnet synchronous motor drive system for electric vehicles using bidirectional z-source inverter', *IET Electr. Syst. Transp.*, 2012, **2**, (4), pp. 178–185

[21] Ellabban, O., Van Mierlo, J., Lataire, P.: 'Direct torque controlled space vector modulated induction motor fed by a Z-source inverter for electric vehicles', 2011 Int. Conf. on Power Engineering, Energy and Electrical Drives, Malaga, 2011, pp. 1–7

[22] Moinoddin, S., Abu-Rub, H., Iqbal, A.: 'Carrier-based PWM of voltage fed five-phase qZSI with coupled inductors', 2013 7th IEEE GCC Conf. and Exhibition (GCC), Doha, 2013, pp. 390–395

[23] Abduallah, A.A., Iqbal, A., Ben-Brahim, L.: 'Space vector pulse width modulation techniques for a five-phase impedance source and quasi impedance source inverters', Industrial Technology (ICIT), 2015 IEEE Int. Conf. on, Seville, 2015, pp. 1173–1178

[24] Abduallah, A.A., Iqbal, A., Meraj, M., *et al.*: 'Discontinuous space vector pulse width modulation techniques for a five-phase quasi Z-source inverter'.

41st Annual Conf. of the IEEE Industrial Electronics Society, IECON 2015, Yokohama, 2015, pp. 4205–4210

[25] Iqbal, A., Moinuddin, S.: 'Comprehensive relationship between carrier-based PWM and space vector PWM in a five-phase VSI', *IEEE Trans. Power Electron.*, 2009, **24**, (10), pp. 2379–2390